The Lipocalin α_1-Microglobulin Has Radical Scavenging Activity*

Bo Åkerström[‡1], **Ghassan J. Maghzal**[§], **Christine C. Winterbourn**[¶], **and Anthony J. Kettle**[¶]

From the ‡Department of Clinical Sciences, Lund University, 22184 Lund, Sweden, the §Centre for Vascular Research, Department of Pathology, Faculty of Medicine, University of Sydney, New South Wales 2006, Australia, and the ¶Free Radical Research Group, Department of Pathology, Christchurch School of Medicine and Health Sciences, Christchurch 8140, New Zealand

The lipocalin α_1-microglobulin (α_1m) is a 26-kDa glycoprotein present in plasma and in interstitial fluids of all tissues. The protein was recently shown to have reductase properties, reducing heme-proteins and other substrates, and was also reported to be involved in binding and scavenging of heme and tryptophan metabolites. To investigate its possible role as a reductant of organic radicals, we have studied the interaction of α_1m with the synthetic radical, 2,2′-azino-bis-(3-ethylbenzthiazoline-6-sulfonic acid) (ABTS radical). The lipocalin readily reacted with the ABTS radical forming reduced ABTS. The apparent rate constant for this reaction was $6.3 \pm 2.5 \times 10^3 \, \text{M}^{-1} \text{s}^{-1}$. A second reaction product with an intense purple color and an absorbance maximum at 550 nm was formed at a similar rate. This was shown by liquid chromatography/mass spectrometry to be derived from covalent attachment of a portion of ABTS radical to tyrosine residues on α_1m. The relative yields of reduced ABTS and the purple ABTS derivative bound to α_1m were ~2:1. Both reactions were dependent on the thiolate group of the cysteine residue in position 34 of the α_1m polypeptide. Our results indicate that α_1m is involved in a sequential reduction of ABTS radicals followed by trapping of these radicals by covalent attachment. In combination with the reported physiological properties of the protein, our results suggest that α_1m may be a radical reductant and scavenger *in vivo.*

The lipocalins are a protein superfamily with 30–35 members distributed among animals, plants, and bacteria (1, 2). The members of the superfamily have a highly conserved three-dimensional structure, 8–9 antiparallel β-strands folded into a barrel with one closed and one open end. The interior of the barrel forms a binding site for small hydrophobic ligands, and this structural property is the basis for a surprisingly wide array of biological functions. So far, three lipocalins have been shown to be enzymes: prostaglandin D-synthase (3), violaxanthin de-

epoxygenase in plants (4), and α_1-microglobulin (α_1m)[2] (5–7), which was recently shown to have reductase/dehydrogenase properties (8).

Also called protein HC (9), α_1m is one of the originally described lipocalins (10) and is one of the most widespread lipocalins phylogenetically (7). So far, it has been found in mammals, birds, fish, and amphibians. The protein is synthesized by the liver (11), rapidly distributed by the blood to the extravascular compartment (12), and found in most organs in interstitial fluids, connective tissue, and basement membranes (13–15). It is especially abundant at interfaces between the cells of the body and the environment, such as in lungs, intestine, kidneys, and placenta (16–18). Due to its small size, 26 kDa, α_1m is rapidly cleared from the blood by glomerular filtration. Most of the filtrated α_1m is degraded in the kidneys, but a small part is excreted in the urine (12). α_1m isolated from plasma and urine is yellow-brown and displays charge heterogeneity (*i.e.* a broad band upon electrophoresis) (19). This is caused by an array of small chromophoric groups attached to the amino acid residues Cys-34, Lys-92, Lys-118, and Lys-130, which are localized around the entrance of the lipocalin pocket (20–22).

The biological function of α_1m is unknown, although it has a number of immunosuppressive properties, such as inhibition of antigen-induced lymphocyte cell proliferation, cytokine secretion (23–25), and the oxidative burst of neutrophils (26). Several recent findings suggest that α_1m is involved in reduction and scavenging of biological pro-oxidants, such as heme and heme-proteins. First, it was shown that α_1m binds heme strongly and obtains the yellow-brown chromophore by incubation with hemoglobin or erythrocyte ghosts, concomitant with degradation of the bound heme (27). A processed form, t-α_1m, which lacks the C-terminal tetrapeptide LIPR and has enhanced heme degradation properties, is also induced by incubation with hemoglobin. t-α_1m is found in urine (27) and continuously forms in chronic leg ulcers, a hemolytic inflammatory condition where free heme and iron are considered to be oxidative pathogenic factors (28). Second, lysyl residues in urine α_1m from hemodialysis patients were found to be modified by kynurenine derivates (29). These are tryptophan catabolites that have a propensity to form free radicals (30–32) and are present at elevated concentrations in plasma of hemodialysis

patients (33). Fourth, α_1m was shown to enzymatically reduce cytochrome *c*, methemoglobin, nitro blue tetrazolium, and free iron, using NADH, NADPH, or ascorbate as electron-donating co-factors (8). The thiol group in position Cys-34 and the three lysyls Lys-92, Lys-118, and Lys-130 were implicated in the active site. Finally, the cellular expression of α_1m is up-regulated by hemoglobin and radical oxygen species (34).

These reports suggest that α_1m could potentially undergo reactions with biological radicals and that these reactions may be related to its physiological function. To investigate how α_1m reacts with radicals, we have studied the interaction of α_1m with the stable radical, 2,2'-azino-bis-(3-ethylbenzthiazoline-6-sulfonic acid) (ABTS). This compound has been used extensively to investigate antioxidant mechanisms (*e.g.* see Ref. 35). We show that α_1m reduces the ABTS radical and simultaneously covalently binds to the radical, forming a distinct purple adduct. The results suggest that the lipocalin α_1m may be a radical reductase and scavenger *in vivo*.

MATERIALS AND METHODS

Proteins and Reagents—Wild type and mutated variants of α_1m were expressed in *Escherichia coli*. Using site-directed mutagenesis, a Cys → Ser substitution was introduced at amino acid position 34 to give the C34S-α_1m mutant (36). In the recombinant α_1m forms, the N terminus was elongated by a 15-amino acid peptide containing eight histidines (His tag) and an enterokinase cleavage site (DDDDKA). The His tag was removed by incubating 10 mg of α_1m with 400 units of enterokinase (Sigma) for 5 h at room temperature in 20 mM Tris-HCl, 0.5 M NaCl, pH 8.0. His tag-free α_1m was then separated from enterokinase by gel chromatography, and the N-terminal amino acid sequence was determined.

Human α_1m was prepared from plasma (37), urine (38), and baculovirus-infected insect cells (39) as described. Human plasma, urine, saliva, and tear fluid were obtained from healthy volunteers. All other proteins and reagents were of analytical grade and were purchased from Sigma if not indicated otherwise.

Alkylation of α_1m—Thiol groups were alkylated by incubating α_1m (0.18 mM) with 22 mM iodoacetamide (IAA) in phosphate-buffered saline (PBS; 10 mM sodium phosphate, pH 7.4, 120 mM NaCl, 3 mM KCl) for 1 h at room temperature in the dark and then dialyzing exhaustively against 25 mM Tris-HCl + 50 mM NaCl, pH 8. Reduced thiol groups were quantified by alkylation with iodo-[^{14}C]acetamide ([^{14}C]IAA) (Amersham Biosciences; specific activity 59.0 mCi (2.2 GBq)/mmol). The reaction mixtures contained 2 μM α_1m in 0.2 M Tris-HCl, pH 8.5, and 1 mM [^{14}C]IAA. The reaction proceeded for 60 min at 25 °C in the dark. To determine the amounts of bound [^{14}C]IAA, the alkylated α_1m was subjected to SDS-PAGE and phosphorimaging.

Reduction of ABTS Radical—A stock solution of ABTS radical was prepared following the procedure of Re *et al.* (40) with minor modifications. Potassium persulfate was added to a 7 mM ABTS solution in water, to a final concentration of 2.8 mM, allowing at least 5 h for the reaction. The solution was kept in the dark and used within 24 h. In some experiments, the amount of potassium persulfate was varied, producing different

ABTS radical/ABTS ratios. The stock solution was diluted 125 times with PBS. α_1m, control proteins, and other reagents were added as described for each experiment, and the reaction was followed by monitoring absorbance changes of ABTS and its radical. End point scanning of the reaction products was done after reducing remaining ABTS radicals by adding NaN$_3$ to a final concentration of 60 mM as described (41). pH studies were done by diluting the stock solution with 20 mM sodium acetate, pH 5.0, or 20 mM sodium phosphate, pH 6.0, 7.0, or 8.0, or 20 mM glycine-OH, pH 9.0.

Estimation of Kinetic Parameters—Initial reaction rates were estimated by linear regression analysis of absorbance values obtained during the first 1 min of the reaction. The total formation of products (*i.e.* the reduced form of ABTS and the purple α_1m modification) and the total consumption of ABTS radical during the initial, rapid reaction phase were determined by linear regression analysis, as illustrated in Fig. 3. K_m and V_{max} values were determined by nonlinear regression of initial reaction rates using different initial α_1m (0.5–4 μM) and ABTS radical (7–55 μM) concentrations and using the same ratio between the initial ABTS radical and ABTS concentrations.

Spectrophotometric Determinations—Spectrophotometric analyses were done either in a Beckman 7500 photodiode array spectrophotometer or a Beckman DU 640i spectrophotometer. The reaction between α_1m and ABTS radical was followed by scanning a 0.5-ml reaction mixture, blanking with PBS or the appropriate dilution buffer. Reading at time 0 was done before the addition of α_1m or control proteins, and at regular time intervals after the addition of the proteins. Concentrations of ABTS were determined by using $\epsilon_{340} = 4.8 \times 10^4 \, \text{M}^{-1} \, \text{cm}^{-1}$ and of the ABTS radical using $\epsilon_{415} = 3.6 \times 10^4 \, \text{M}^{-1} \, \text{cm}^{-1}$ (42). Concentrations of α_1m were determined by using the extinction coefficients at 280 nm reported for urine, plasma, and baculovirus-infected insect cell α_1m (39) and $3.6 \times 10^4 \, \text{M}^{-1} \, \text{cm}^{-1}$ for recombinant α_1m. The absorbance values at 550 nm at different time points (A_{550}) were calculated after correction for spillover absorbance of the ABTS radical using the following formula: $A_{550} = 0.5 \times (A_{550}(\text{observed}) - 0.403 \times A_{735}) + 0.5 \times (A_{550}(\text{observed}) - 0.163 \times A_{415})$. The coefficients in this equation were determined by absorbance scanning of the ABTS radical at known concentrations.

Purification of Purple α_1m—The purple end product of α_1m was purified by gel filtration. α_1m (80–140 μM) was incubated for 5 min with the ABTS radical/ABTS stock solution (1.2–1.8 mM) in PBS. After centrifugation at 8000 $\times$ *g* for 2 min, the reaction product was applied to a 1-ml column packed with Sephadex G-25 Fine and equilibrated with 2 mM NH$_4$HCO$_3$, pH 8.5. The column was eluted with the equilibration buffer at free flow, and 0.2-ml fractions were collected manually. The eluted fractions were analyzed by absorbance scanning. Protein-containing fractions were pooled.

SDS-PAGE, Blotting, and N-terminal Sequence Analysis—SDS-PAGE was performed using 12% gels in the buffer system described by Laemmli (43), with or without 2% (v/v) β-mercaptoethanol in the sample buffers. High molecular mass standards (Rainbow markers; Amersham Biosciences) were used. N-terminal amino acid sequence analysis was achieved by Edman degradation (Protein Analysis Center, KI, Stockholm, Sweden)

of bands separated by SDS-PAGE and transfer to polyvinylidene difluoride membranes (Immobilon-P, Millipore, Bedford, MA) as described (44).

Reaction of ABTS Radical with Tyrosine—ABTS radicals were generated by using hydrogen peroxide (50 μM) and lactoperoxidase (5 μg/ml) to oxidize ABTS (100 μM) in 50 mM phosphate buffer, pH 7.4. When the formation of ABTS radicals reached a maximum (approximately 35 μM), catalase (10 μg/ml) was added to scavenge residual hydrogen peroxide. Tyrosine (10–30 μM) was then reacted with the ABTS radicals. It caused a stoichiometric loss in ABTS radicals within 5 min and promoted the formation of a product that had an absorbance maximum from 500 to 550 nm. This final reaction mixture was analyzed by LC/MS as described below.

Reaction of α_1m with Glycyl-Tyrosyl Radicals—Radicals of the Gly-Tyr peptide were generated using lactoperoxidase and hydrogen peroxide. Reactions were carried out in 10 mM phosphate buffer, pH 7.8, containing 140 mM NaCl, 20 μM Gly-Tyr, 25 μg/ml lactoperoxidase, and 10 μM diethylenetriaminepentaacetic acid with or without α_1m, orosomucoid, or HSA. They were started by adding 5 μM hydrogen peroxide. After 30 min at 20 °C, the fluorescence due to formation of dityrosine was measured (λ_{ex}, 325 nm; λ_{em}, 405 nm) in a Jasco J-810 Spectrofluorimeter (Jasco Scandinavia AB, Mölndal, Sweden).

Preparation of Protease Fragments of α_1m after Reaction with ABTS Radicals—ABTS and α_1m were reacted and desalted as described previously to generate the purple product. After boiling for 2 min, Pronase (Protease XIV from *Streptomyces griseus*) at a 1:25 enzyme/substrate ratio was added to the ABTS-α_1m and incubated at 37 °C for 2 h. Alternatively, trypsin was added at a ratio of 1:10 and incubated at 37 °C for 3 h. The digests were then subjected to HPLC separation on a Phenomenex Luna 5μ C18 column (250 × 4.6 mm) using the following stepwise gradient. From 0 to 5 min, the eluent was 100% solvent A (10% methanol in 50 mM phosphate buffer, pH 6.5, containing 2.5 mM *n*-octylamine); the organic phase was then increased to 50% over the following 5 min and kept at 50% between 10 and 30 min. The flow rate was 0.8 ml/min. Peaks that absorbed at 550 nm were well resolved from ABTS and ABTS radical. They were collected for subsequent analysis by LC/MS.

Liquid Chromatography-Mass Spectrometry Analysis of α_1m Digests—Tryptic peptides were analyzed by LC/MS by selecting and fragmenting major ions that eluted in the chromatogram. Peptides that contained ABTS were identified by the presence of an absorbance maximum around 550 nm and characteristic molecular fragments of ABTS in the MS/MS spectrum. The purple digestion products of the ABTS-α_1m were separated on a Jupiter Proteo column (particle size 4 μm, 150 × 2.0 mm) (Phenomenex, Torrance, CA), using a Surveyor HPLC pump (Thermo Corp., San Jose, CA). The column was maintained at 30 °C. The products were eluted at a flow rate of 0.2 ml/min using a linear gradient of two solvents: solvent A (0.1% formic acid) and solvent B (0.1% formic acid, 90% acetonitrile). The gradient was as follows: 0–30 min, increased solvent B to 50%; 30–32 min, increased solvent B to 100%; 32–34 min, maintained solvent B at 100%; 34–35 min, decreased solvent B to 0%. The injection volume was 20 μl. The HPLC was coupled to an ion trap mass spectrometer (ThermoFinnigan LCQ Deca XP
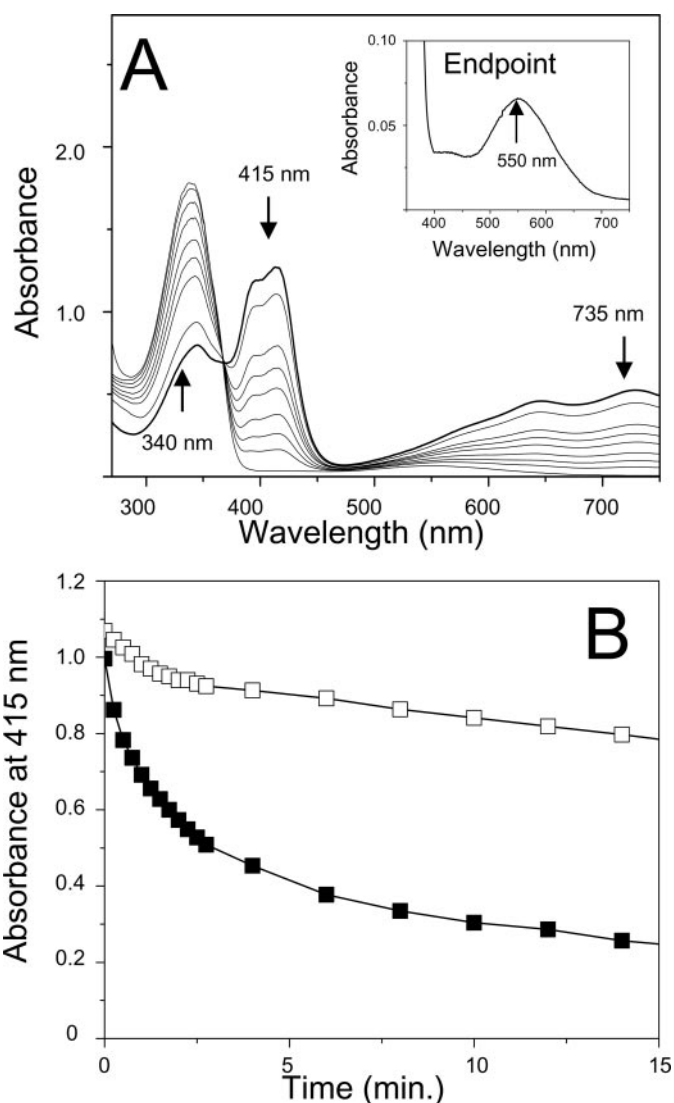

FIGURE 1. **Reaction between α_1m and ABTS radical.** A solution containing 36 μM ABTS radical and 18 μM ABTS was prepared by incubating 2.8 mM potassium disulfite with 7 mM ABTS for 24 h and diluting with PBS, and α_1m was added to 3.5 μM. *A*, the absorbance spectrum was read at 0 s (*i.e.* before the addition of α_1m), 2 s, 30 s, 1 min, 2 min, 5 min, 10 min, and 20 min. Sodium azide was added to 60 mM to reduce the remaining ABTS radicals, and the end point scan was read (end point scan and *inset*). *B*, the absorbance at 415 nm was read at regular time intervals after adding a 4 μM concentration of either α_1m (■) or HSA (□) to 30 μM ABTS radical in PBS.

Plus; Thermo Corp.) equipped with an electrospray ionization source. The mass spectrometer was operated with positive ionization using full scan mode (scan range 100–2000 m/z). Spray voltage was set at 3.5 kV, the capillary temperature was set at 275 °C, and the sheath gas flow was set at 35 units (instrument units). For MS/MS experiments, parent ions were fragmented in the ion trap using 35% collision-induced energy.

RESULTS

Reaction between α_1m and ABTS Radical—The ABTS radical was readily reduced by α_1m (Fig. 1). Overlaid scans of the solution show a decrease of the ABTS radical-specific 415 and 735 nm peaks and a concomitant increase of the ABTS-specific peak at 340 nm. An almost complete reduction was seen after
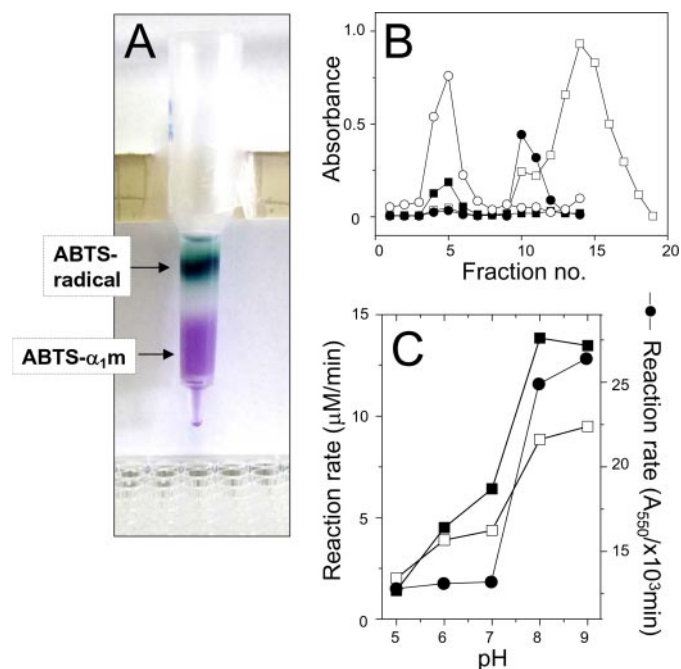
FIGURE 2. **Preparation of ABTS-α_1m (*A* and *B*) and pH dependence of the reaction between α_1m and ABTS radical (*C*).** α_1m was added (final concentration 0.14 mM) to ABTS radical (1.7 mM) and ABTS (0.8 mM) in 60 mM Tris-HCl, pH 8, 0.5 M NaCl and incubated for 5 min. To illustrate the separation, fresh ABTS radical was then added to 1 μM. *A*, the reaction mixture was applied to a 2-ml column packed with Sephadex G-25 Fine and eluted with 2 mM NH_4HCO_3, pH 8.5. The positions of the *green* ABTS radical and the *purple* ABTS-α_1m are indicated by *arrows*. *B*, fractions were collected and analyzed by reading the absorbance spectrum. The absorbance values at 280 nm (■), 340 nm (□), 415 nm (●), and 10 × 550 nm (○) of each fraction were plotted. *C*, the reaction of 2 μM α_1m with the standard ABTS radical/ABTS solution was followed at various pH values by monitoring the absorbance at 340, 415, and 550 nm over 20 min. The initial rates of ABTS radical consumption (■), ABTS formation (□), and formation of *purple* product (A_{550}) (●) were determined as described under "Materials and Methods."

20 min by 3.5 μM α_1m (Fig. 1*A*). Remaining ABTS radicals were reduced by adding 60 mM NaN_3, revealing two end products, reduced ABTS, represented by the 340 nm peak, and a novel peak at 550 nm (Fig. 1*A*, *inset*), which gave the solution a purple color. Two separate phases of the reaction could be distinguished (Fig. 1*B*), an initial faster phase over the first 5 min and a second slower phase that was still ongoing after 2 h. A clear difference in the rate of the first phase was seen between α_1m and HSA (Fig. 1*B*) as well as the control proteins ovalbumin, orosomucoid, and soybean trypsin inhibitor (not shown). In contrast, the rate of the second phase was similar between α_1m and the control proteins. Thus, the second phase was regarded as nonspecific and is not discussed further. After 5 min, ~8–9 ABTS radical molecules had been consumed per molecule of α_1m. Trolox, a water-soluble analogue of vitamin E, reduced ABTS radical stoichiometrically at a 1:1 molar ratio (not shown).

To study the reaction products, 1 mg of α_1m was allowed to react with a ~10–12-fold excess of ABTS radicals for 5 min, applied to a Sephadex G-25 column, and eluted, and fractions were collected (Fig. 2, *A* and *B*). The purple product (*i.e.* the absorbance at 550 nm) co-eluted with the α_1m protein (absorbance at 280 nm), whereas remaining ABTS radicals and ABTS were eluted later.

The pH dependence of the reactions was investigated between pH 5 and 9 using standard conditions (Fig. 2*C*). A slow rate of ABTS radical consumption and formation of reduced ABTS was seen at pH 5, the rates increased between pH 5 and 8, and no further increase was seen at pH 9. This suggests possible involvement of cysteine, tyrosine, or histidine residues on α_1m, side chains on which deprotonization is likely to occur between pH 5 and 8. A much more striking pH dependence was seen for the formation of the purple ABTS-α_1m. The absence of reaction below pH 7 and a sharp increase in the rate between pH 7

TABLE 1

Reaction rates in various physiological media of 2.5 μM α_1m and the standard ABTS radical/ABTS solution

Medium	Initial rate of ABTS radical loss[a]		
	50×[b]	100×	200×
		μM/s	
Buffer[c]		0.37 (0.02)[d]	
Plasma		0.34 (0.05)	
Urine		0.35 (0.04)	
Saliva	0.33 (0.04)	0.36 (0.03)	0.37 (0.05)
Tear fluid	0.38 (0.03)	0.43 (0.04)	0.41 (0.03)

[a] Calculated as described under "Materials and Methods," subtracting the rate of ABTS radical loss in the absence of α_1m.
[b] Factor dilution of medium with buffer.
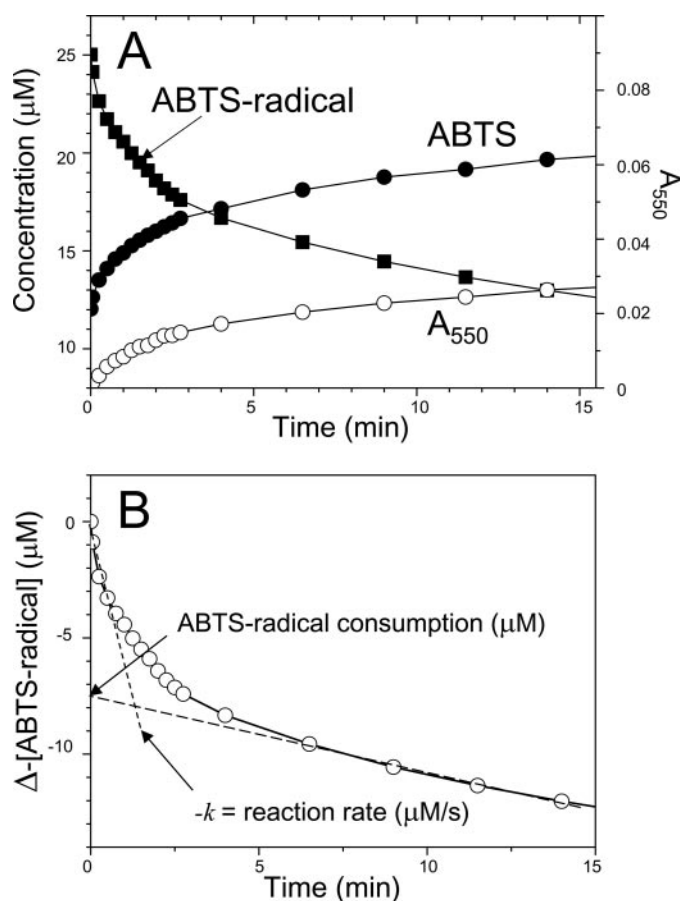[c] 20 mM sodium phosphate, pH 8.0.
[d] Mean ± S.D. ($n = 3$).

FIGURE 3. **Kinetics of the reactions between α_1m and ABTS radical.** *A*, the reaction of 1 μM α_1m with the standard ABTS radical/ABTS solution was followed by reading the absorbance and the concentration of the ABTS radical, ABTS, and A_{550}. *B*, the net loss of ABTS radical was plotted from the experiment in *A*. The initial reaction rate and end point ABTS radical consumption during the initial rapid reaction phase were estimated as shown in the figure.
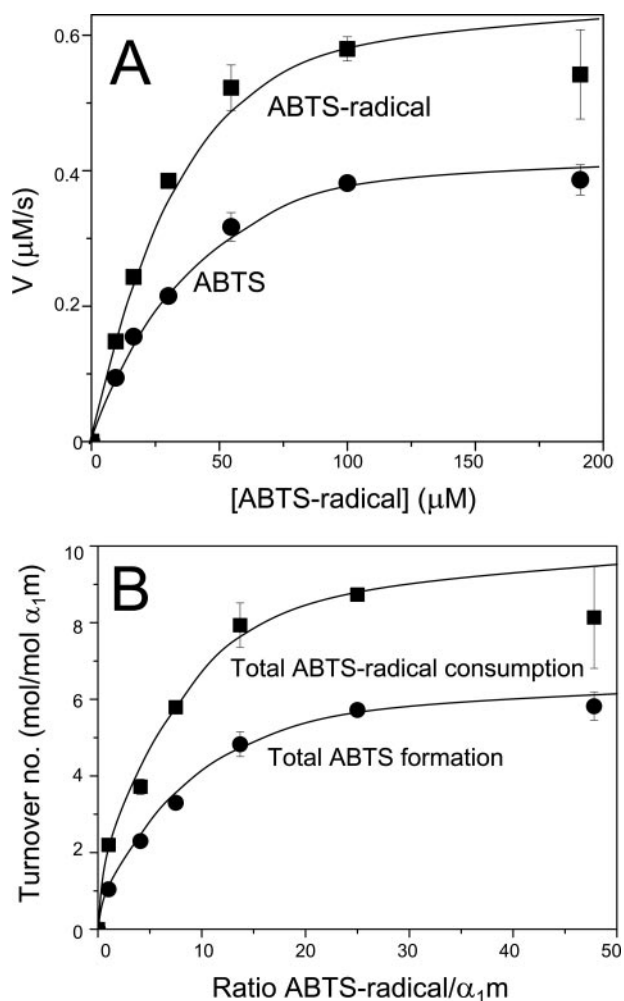
FIGURE 4. **Reaction rates, ABTS radical consumption, and ABTS formation at various ABTS radical concentrations.** The reaction of 0.5–4 μM α_1m with the standard ABTS radical/ABTS solution at different dilutions was followed by reading the absorbance spectra at different time points. *A*, the initial reaction rates (*V*) of ABTS radical loss (■) and ABTS formation (○) were plotted as a function of the initial concentration of ABTS radical ([S]), relative to 4 μM α_1m. *B*, the end point ABTS radical consumption and ABTS formation, as described in the legend to Fig. 3*B*, were plotted as a function of the ratio ABTS radical/α_1m concentrations. Each point represents the mean of triplicates ± S.D.
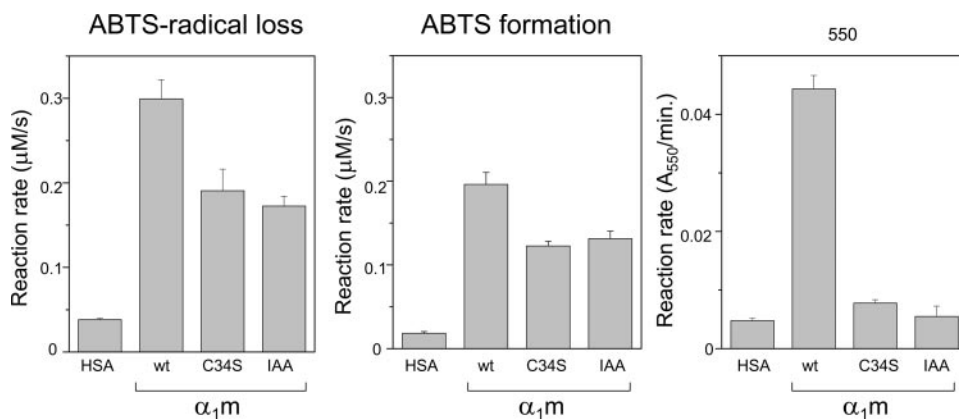

FIGURE 5. **Influence of the Cys-34 thiol group of α_1m on the reaction with ABTS radical.** The reaction of 2 μM wild type (*wt*), C34S, alkylated (*IAA*) α_1m, or HSA with the standard ABTS radical/ABTS solution was followed by reading the absorbance spectra at different time points. The initial rates of the ABTS radical consumption, ABTS formation, and absorbance at 550 nm were calculated as described in the legend to Fig. 5*B*. Each *bar* represents the mean ± S.D. of triplicate experiments.

and 8 suggest involvement of side groups with a pK_a around 7.5. The His tag of the recombinant α_1m did not influence the rates of ABTS radical consumption or formation of ABTS-α_1m (not shown). This was supported by experiments using plasma and urine α_1m, which lack the His tag (see below). The addition of 0.25–1 μM superoxide dismutase did not slow down the consumption of the ABTS radical or the formation of ABTS-α_1m (not shown), suggesting that superoxide radicals were not involved.

The rate of ABTS radical loss during the first 60 s of the reaction was estimated in various body fluids (Table 1). The decay of the radical in the absence of α_1m was substantial in most fluids, but at higher dilutions, this could be subtracted from the loss induced by α_1m. As shown in Table 1, similar rates are seen in plasma, urine, saliva, and tear fluid, suggesting that similar reactions may occur *in vivo*. Furthermore, similar rates are seen at various dilutions of saliva and tear fluid.

Kinetics and Stoichiometry—The formation of ABTS-α_1m coincided in time with the consumption of ABTS radicals and formation of reduced ABTS (Fig. 3*A*). This suggests that the three reactions are linked. Fig. 3*B* illustrates how the rate of the consumption of the ABTS radical and the total consumption of ABTS radical were calculated. The same method was employed to calculate the corresponding parameters for the formation of reduced ABTS and the purple ABTS-α_1m.

The reaction rates for ABTS radical consumption, ABTS formation, and production of ABTS-α_1m (A_{550}), calculated as described in the legend to Fig. 3*B*, were determined at different initial concentrations of the ABTS radical and ABTS. The rate of formation of ABTS-α_1m (A_{550}) was independent of the initial ABTS radical and ABTS concentrations (not shown). However, both the rate of ABTS radical consumption and rate of ABTS formation increased to a maximum with increasing initial concentration of ABTS radical (Fig. 4*A*). The plots show that the rate of consumption of ABTS radical exceeded the rate of formation of reduced ABTS. The V_{max} and K_m values for the loss of ABTS radicals were calculated by nonlinear regression to be 0.68 ± 0.06 μM s^{-1} and 27.2 ± 8.1 μM, respectively. These gave a first order rate constant ($V_{max}/[\alpha_1$m]) for reaction of ABTS radical with α_1m of 0.17 ± 0.02 s^{-1} and an apparent second order rate constant (V_{max}/K_m or k_{app}) for reduction of ABTS radicals of 6.3 ± 2.5 × 10^3 M^{-1} s^{-1}.

The total ABTS radical consumption and total ABTS formation were plotted as functions of the initial ABTS radical concentration (Fig. 4*B*). This demonstrated that 8–9 ABTS radical molecules were consumed per α_1m molecule, and six ABTS molecules were formed during the first phase of the reaction. This also suggests that up to 2–3 molecules of ABTS were bound to each molecule of α_1m (*i.e.* the amount of ABTS radicals not converted to reduced ABTS).
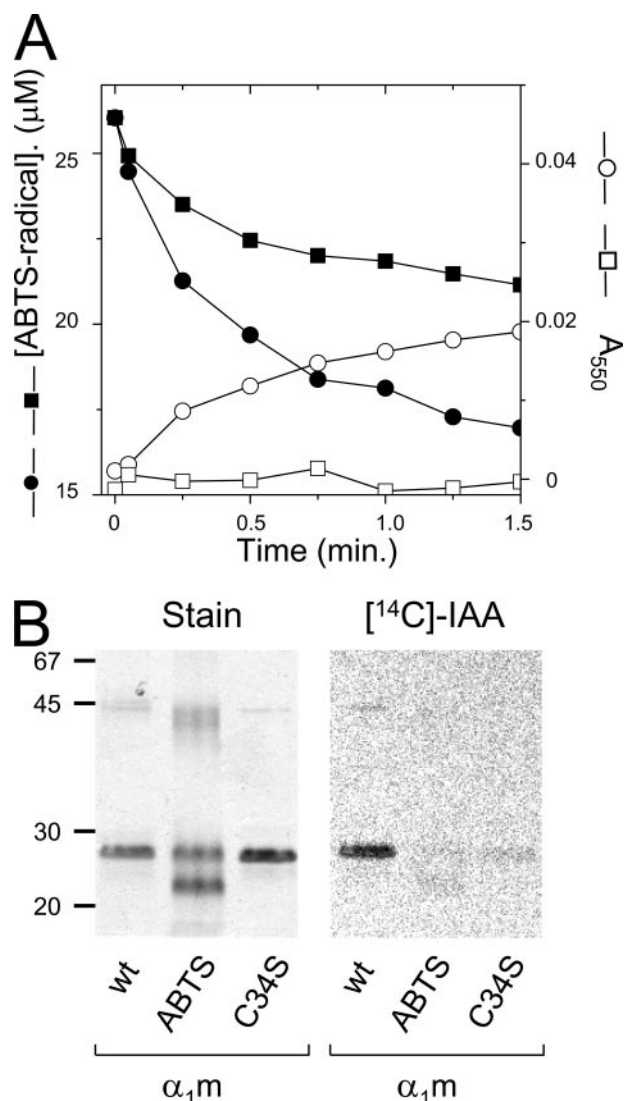
FIGURE 6. **Reactions with ABTS radical of preformed ABTS-α_1m (*A*) and analysis of the free thiol of ABTS-α_1m (*B*).** *A*, the reaction of 2 μM α_1m (*circles*) or 2 μM desalted ABTS-α_1m (*squares*) with the standard ABTS radical/ABTS solution was followed by reading the absorbance spectra at different time points. The readings were blanked with the protein solutions, respectively, without ABTS radical or ABTS, before plotting. *B*, alkylation with [^{14}C]IAA and separation by SDS-PAGE. Recombinant wild type α_1m (1 μg) (*wt*), C34S-α_1m (1 μg), or ABTS-α_1m (2 μg) was incubated with [^{14}C]IAA as described under "Materials and Methods" and then separated by SDS-PAGE under reducing conditions. The gels were protein-stained (*Stain*) and analyzed for radioactivity by phosphorimaging ([^{14}C]IAA).

FIGURE 7. **Analysis of the Pronase digest of ABTS-α_1m using LC/MS.** ABTS-α_1m was digested with Pronase, and the purple products were isolated by gel filtration (see "Materials and Methods") and then separated by HPLC (*A*). *B*, the absorption spectrum of peak 1. *C*, the mass spectrum of peak 1, indicating the major ion at 451 *m/z*. *D*, the MS/MS spectrum of the 451 *m/z* ion in peak 1 was obtained using 35% collision energy for fragmentation. *E*, the MS/MS spectrum of ABTS radical using 35% collision energy.

Reactions with Various α_1m Forms and Mutants—The reactions of recombinant α_1m were compared with those of α_1m purified from human plasma and urine and recombinant α_1m from baculovirus-infected insect cells. No significant differences in any of the reaction rates were found between the α_1m forms (not shown). The influence of the Cys-34 thiol group was studied using the mutated α_1m variant C34S-α_1m and alkylated α_1m (IAA-α_1m) (Fig. 5). A significant, but incomplete, decrease of the reduction rate of ABTS radical was seen between the wild type protein and the two thiol group-modified variants. The formation of the purple ABTS-α_1m was decreased to background levels using C34S- and IAA-α_1m. This suggests that the Cys-34 thiol group is essential for the binding of ABTS to the
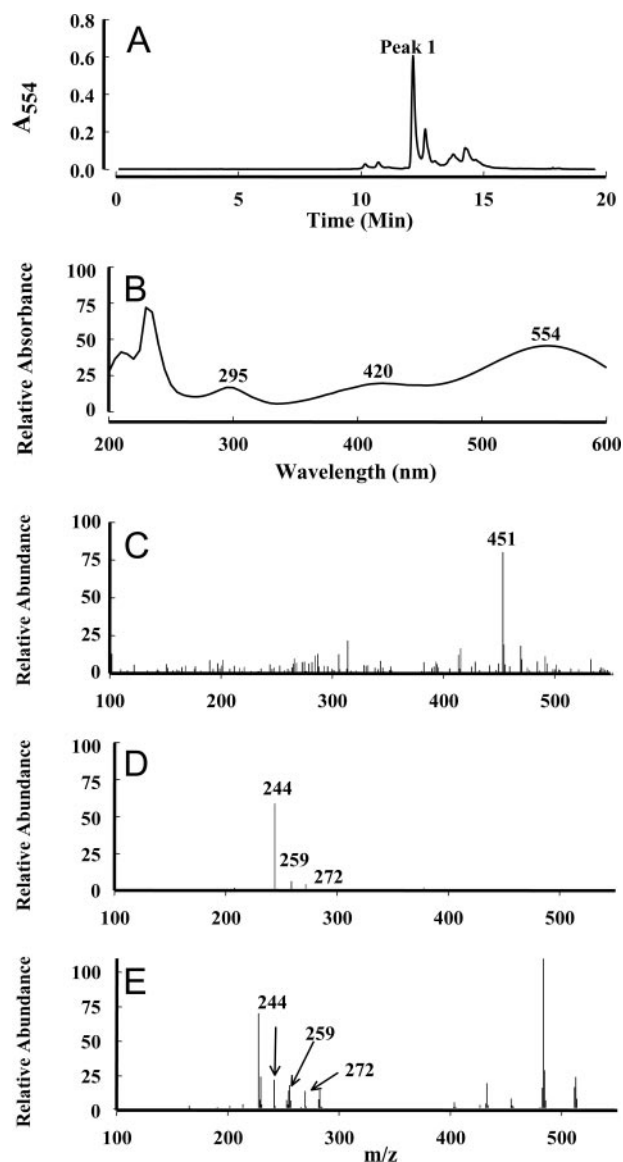
protein and is also involved in the reduction of the ABTS radical.

Molecular Characterization of ABTS-α_1m—The purified and desalted ABTS-α_1m was allowed to react with a solution of ABTS radical (Fig. 6*A*). The ABTS-α_1m reduced the ABTS radical at a decreased rate compared with α_1m. No more purple color was formed. This suggests that the binding of ABTS on the α_1m molecule is saturable (*i.e.* only a limited number of positions on α_1m can be modified) and that the sites for the two reactions are partially linked.

SDS-PAGE shows two major molecular forms of ABTS-α_1m, 28 and 24 kDa, and the presence of small amounts of a higher molecular weight band (Fig. 6*B*). A large aggregate was seen in both unreacted wild type α_1m and ABTS-α_1m. The same pat-
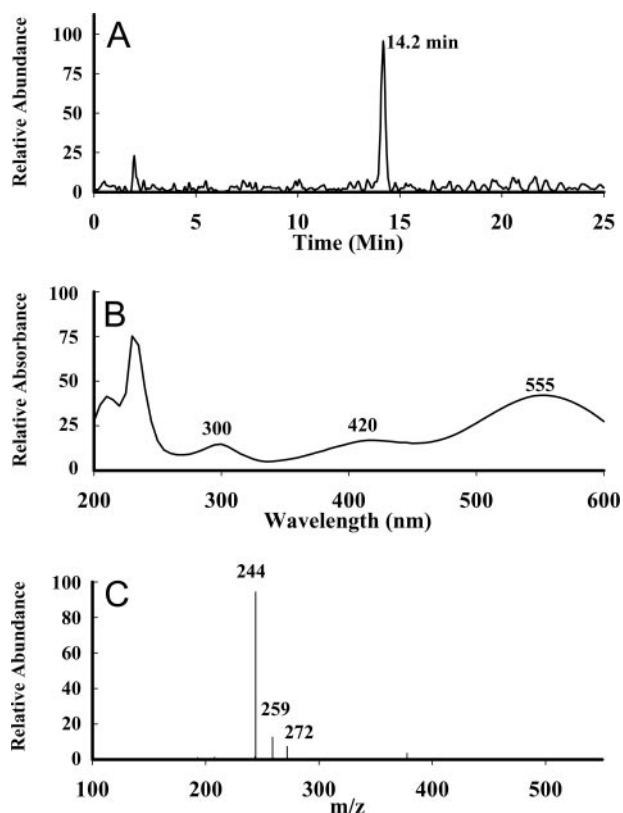
FIGURE 8. **LC/MS analysis of the product formed from the reaction of ABTS radical with tyrosine.** *A*, ABTS radical was reacted with tyrosine (see "Materials and Methods"), and the reaction mixture was analyzed by LC/MS by selectively monitoring ions with an *m/z* of 451 mass units. *B*, the absorption spectrum of the peak eluting at 14.2 min. *C*, the MS/MS spectrum of 451 *m/z* ions in the peak eluting at 14.2 min, using 35% collision energy for fragmentation.
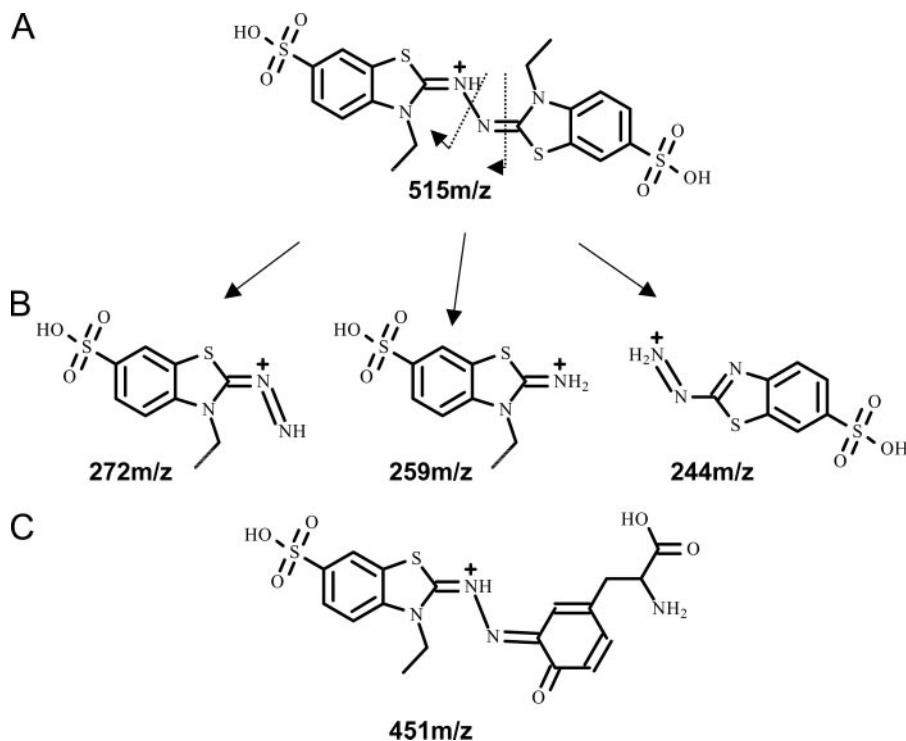

FIGURE 9. *A*, the structure of ABTS radical [M + H] ion. *B*, theoretical structures of the MS/MS fragments derived from ABTS radical [M + H] ions and also found in the MS/MS spectra of ABTS-α_1m Pronase and trypsin digests. *C*, proposed structure of the ABTS-tyrosine conjugate [M + H] ion.

tern was obtained without reducing agents in the gel (not shown). The N-terminal sequence of the 24-kDa band was AGPVPT, corresponding to the native protein without the N-terminal His$_8$ tag and enterokinase cleavage site, but with an extra N-terminal alanine. Alkylation of the Cys-34 residue with radiolabeled iodoacetamide showed incorporation to wild type α_1m but not to ABTS-α_1m (Fig. 6*B*). As expected, C34S-α_1m was negative. This demonstrates that the thiol group of ABTS-α_1m was completely modified. The purple color of ABTS-α_1m could be reduced by a large excess of dithiothreitol, and no spectral evidence of any reduced ABTS or ABTS radical was obtained (not shown). This suggests that the purple product is an oxidized form of ABTS and is covalently linked to the protein moiety.

Identification of Purple Modifications on ABTS-α_1m—Pronase digestion of ABTS-α_1m and subsequent purification by HPLC gave two peaks with absorbance at approximately 550 nm. The major peak (Fig. 7, *A* and *B*) had a dominant ion of 451 *m/z* (Fig. 7*C*). Its MS/MS spectrum (Fig. 7*D*) had three molecular fragments in common with those of the mass spectrum of the ABTS radical (Fig. 7*E*). The structure of ABTS and these three fragments are shown in Fig. 9, *A* and *B*. The results of this experiment confirm that the purple product contained ABTS or a part of the ABTS molecule.

It has been shown that phenols react with ABTS radicals to form purple compounds with broad absorbance around 550 nm (40, 44). Therefore, we reacted tyrosine with ABTS radical and analyzed the resulting reaction mixture by LC/MS (Fig. 8). It contained a species with a mass of 451 *m/z* that had an absorbance maximum at 555 nm (Fig. 8, *A* and *B*). The mass spectrum of this compound contained three molecular fragments (Fig. 8*C*) in common with the ABTS radical (Fig. 7*E*) and the purple product obtained from ABTS-α_1m (Fig. 7*D*). These results indicate that ABTS radicals react with tyrosyl residues on α_1m to form the purple product that has a mass of 451 *m/z*. Based on these results and the MS/MS spectra, a structure for the ABTS-Tyr adduct is shown in Fig. 9*C*.

Several tryptic peptides were identified that absorbed at 550 nm. Two of these could be matched to expected tryptic peptides of unmodified α_1m. These two peptides were present in the first fraction from the initial HPLC purification, and they eluted at 13.5 and 14.2 min after subsequent separation by LC/MS (Fig. 10, *A* and *B*). They had major ions with *m/z* ratios of 375.2 (Fig. 10*C*) and 389.1 mass units (Fig. 10*D*), respectively. The mass spectra also contained ions with *m/z* ratios of 749.1 (Fig. 10*C*) and 777.1 (Fig. 10*D*) mass units, respectively. These respective ions had the correct *m/z* ratios to
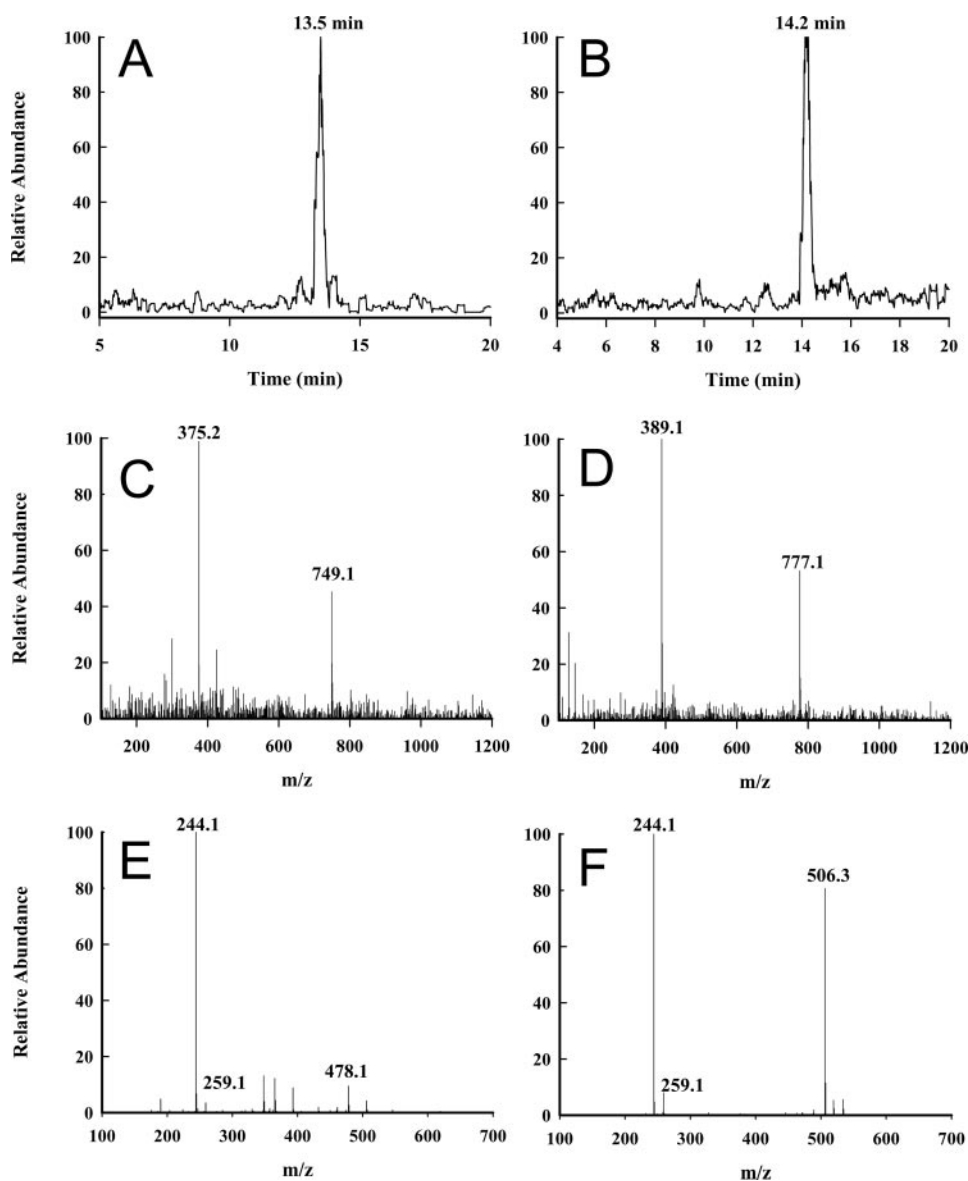
FIGURE 10. **Analysis of a tryptic peptide of ABTS-α_1m using LC/MS.** The first fraction of purple ABTS-α_1m tryptic peptides that was isolated by HPLC was subjected to LC/MS analysis. The first (*A*) and second (*B*) purple peptides eluted at 13.5 and 14.2 min, respectively, and had *m/z* ratios of 375.2 and 389.1 mass units, respectively. *C*, the mass spectrum of the peptide eluting at 13.5 min. *D*, the mass spectrum of the peptide eluting at 14.2 min. *E*, the MS/MS spectrum of the 375.2 *m/z* ion, obtained using 35% collision energy for fragmentation. *F*, the MS/MS spectrum of the 389.1 *m/z* ion was obtained using 35% collision energy for fragmentation.

(Fig. 10*F*) in the respective MS/MS spectra of the doubly charged species. These fragments would arise from the loss of the ABTS portion of the modified peptides, which would give ions 2 mass units less than the unmodified peptides due to oxidation of the tyrosine residues. The presence of ions with *m/z* ratios of 244.1 and 259.1 mass units confirms that a portion of ABTS was present in the peptides (*cf.* Fig. 7). From this finding, it is apparent that ABTS reacts with at least two tyrosine residues in α_1m to form covalent adducts.

Reaction of α_1m with Glycyl-Tyrosyl Radicals—We determined whether α_1m can react with other physiologically relevant free radicals. Radicals of the dipeptide Gly-Tyr were generated using lactoperoxidase and hydrogen peroxide (45). Upon adding hydrogen peroxide to the dipeptide and lactoperoxidase, fluorescence associated with dityrosine-like products was produced and was prevented by α_1m in a concentration-dependent manner (Fig. 11). Neither human serum albumin nor orosomucoid inhibited the fluorescence. Thus, we conclude that α_1m reacts with a transient oxidant formed during oxidation of Gly-Tyr and that this reaction is not a general activity of proteins.

DISCUSSION

In this investigation, we have demonstrated that the lipocalin α_1m rapidly reacts with the ABTS radical by reduction and covalent binding of ABTS derivatives to tyrosine residues in its polypeptide chain. This activity is superstoichiometric, because one molecule of α_1m was capable of scavenging 8–9 molecules of the ABTS radical. Furthermore, the rate of reduction of ABTS radical by α_1m displayed saturation kinetics, which indicates that the ABTS radical must bind to α_1m before it is reduced. Based on the results of the kinetic experiments, we propose that the following reactions are predominant,

$$ABTS^{\bar{\cdot}} + \alpha_1 m \leftrightarrows ABTS^{\bar{\cdot}} \alpha_1 m$$

$$ABTS^{\bar{\cdot}} \alpha_1 m \leftrightarrows ABTS^{2-} + \alpha_1 m^{\dot{+}}$$

$$ABTS^{\bar{\cdot}} + \alpha_1 m^{\dot{+}} \rightarrow ABTS\text{-}\alpha_1 m$$

indicate that the major ions were a doubly charged species. Thus, the masses of the ABTS-containing peptides were 749.1 and 777.1 mass units.

We calculated masses for the unmodified peptides that form ABTS adducts by subtracting 269 mass units from the singly charged peptides. The value of 269 *m/z* was obtained from the ABTS part of the ABTS-Tyr adduct (271 *m/z*) minus two mass units that account for the oxidized tyrosine residue. The calculated masses for the unmodified peptide were 480.1 and 508.1 mass units, respectively. These masses correspond to the predicted tryptic peptides IYGK (480.3) and LYGR (508.3), corresponding to tyrosine residues Tyr-22 and Tyr-132, respectively.
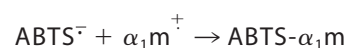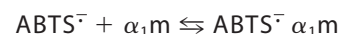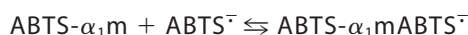
Confirmatory evidence that supports these assignments was the presence of ions with *m/z* ratios of 478.1 (Fig. 10*E*) and 506.3

$$ABTS\text{-}\alpha_1m + ABTS^{\overline{\cdot}} \leftrightarrows ABTS\text{-}\alpha_1mABTS^{\overline{\cdot}}$$

$$ABTS\text{-}\alpha_1mABTS^{\overline{\cdot}} \leftrightarrows ABTS\text{-}\alpha_1m^{\overset{+}{\cdot}} + ABTS^{2-}$$

$$ABTS\text{-}\alpha_1m^{\overset{+}{\cdot}} + ABTS^{\overline{\cdot}} \rightarrow (ABTS)_2\text{-}\alpha_1m$$

REACTIONS 1–6

where $ABTS^{\overline{\cdot}}$ represents the ABTS radical, $ABTS^{2-}$ represents reduced ABTS, and $ABTS\text{-}\alpha_1m$ represents the purple product.
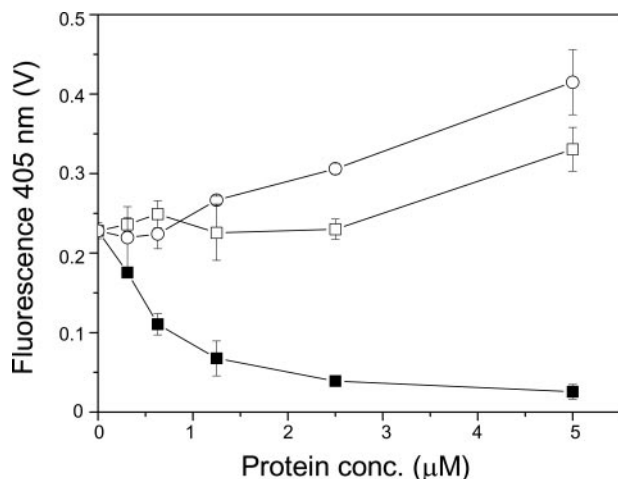

FIGURE 11. **Inhibition of Gly-Tyr dimer formation.** Gly-Tyr peptide (20 μM), diethylenetriaminepentaacetic acid (*DTPA*) (10 μM), lactoperoxidase (25 μg/ml), and hydrogen peroxide (5 μM) were incubated with dilution series of α_1m (■), HSA (○), or orosomucoid (□) in 0.2 ml of 10 mM sodium phosphate buffer, pH 7.8, 0.14 M NaCl, at 20 °C. The fluorescence at 405 nm was read (excitation 325 nm) after 30 min. Each point represents the mean ± S.D. of duplicate experiments.
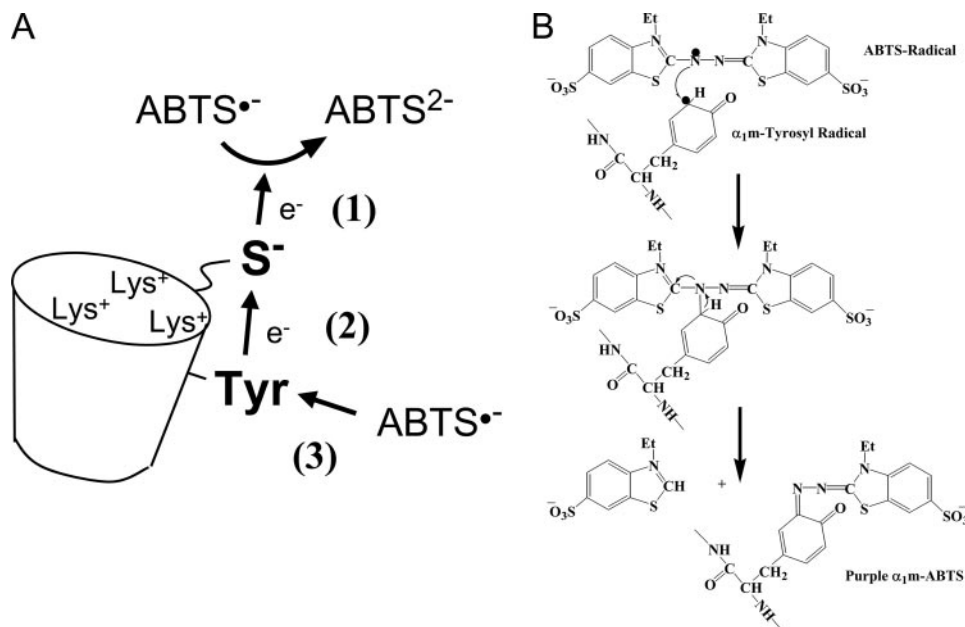

FIGURE 12. **Tentative mechanism of the reactions between α_1m and ABTS radical.** *A*, α_1m is represented by a lipocalin barrel with Tyr-132 and the thiolate group of Cys-34 highlighted. The latter is located on a large, flexible loop (Ω-loop). The pK_a of the Cys-34 thiolate is lowered by the proximity of the three positively charged side chains of Lys-92, Lys-118, and Lys-130, located near the Ω-loop. *1*, the C34 thiolate group reacts with ABTS radical, and a thiyl radical and reduced ABTS are formed. *2*, the thiolate is regenerated by an intramolecular reaction with tyrosine residues, including Tyr-132 and -22, producing a tyrosyl radical. *3*, subsequently, the tyrosyl radical reacts with the ABTS radical, forming a stable purple Tyr-ABTS adduct. *B*, proposed detailed reaction scheme of *reaction 3* of *A*.

The results demonstrated that 8–9 ABTS radicals were consumed per α_1m molecule, but only 5–6 reduced ABTS molecules formed during the first phase of the reaction. This suggests that 2–3 molecules of ABTS were bound to each molecule of α_1m (*i.e.* the amount of ABTS radicals not converted to reduced ABTS). The purple ABTS conjugation products were localized to at least two different tyrosine residues, Tyr-22 and Tyr-132, supporting the possibility that several ABTS residues can be covalently linked to the same α_1m molecule. It is also possible that ABTS conjugation products may be linked to additional locations besides Tyr-22 and Tyr-132, because not all of the purple Pronase and trypsin ABTS-α_1m digestion products could be identified.

Based on the products formed in the analogous reactions of ABTS radical with *p*-hydroxybenzoic acid (41) and the plant flavonoid naringin (46), we propose that a tyrosyl radical on α_1m reacts with the ABTS radical via the reaction shown in Fig. 12*B*. The product formed in this reaction has the required molecular mass of 451 *m/z* for the product identified when the purple α_1m protein was digested with Pronase.

We propose a tentative reaction scenario for radical scavenging by α_1m (see Fig. 12*A*) based on the above reactions and the recent finding that α_1m has catalytic reductase properties, involving the unpaired thiol group of Cys-34 in the reactive center (8). However, our experiments with the alkylation of the Cys-34 thiol plus its mutation to a serine residue demonstrated that Cys-34 was not solely responsible for reduction of ABTS radicals. This result invokes two possible explanations for the reductant activity of α_1m. Either an unidentified residue reduces ABTS radicals and its reductant activity is optimized by Cys-34, or an unidentified residue and Cys-34 both reduce ABTS radicals. Reaction of the cysteine thiol is expected to be favorable, because cysteine reduces the ABTS radical with a second order rate constant of 1.9×10^6 M^{-1} s^{-1} (47). The value of k_{app} for reduction of ABTS radicals by α_1m that we obtained was 300-fold less than this rate constant. However, this is expected, because k_{app} will be a function of the rate constants for the reversible reaction between ABTS radical and the thiol group plus that for binding of ABTS radical to α_1m.

Once the incipient radicals are formed on the α_1m, they must become localized to Cys-34, which in turn oxidizes tyrosine residues to tyrosyl radicals. These tyrosyl radicals would then covalently couple with the ABTS radical to form the purple adduct (Fig. 12). This proposal is supported by our finding that the purple adduct was formed only when the Cys-34 thiol group was present in the protein. Further-

more, cysteine thiyl radicals are capable of one-electron oxidation of tyrosine residues (48). The reaction of the thiyl radical with tyrosine residues need not be direct, because tyrosine residues can be the ultimate sink for oxidizing equivalents in proteins (49), which reflects the thermodynamic pecking order of free radicals (50). Reduction of the thiyl radicals by tyrosine residues is a repair reaction that enables superstoichiometric scavenging of ABTS radicals. Thus, we have compelling evidence that when radicals are formed on α_1m, they are transferred through the protein and localized to tyrosyl residues. Analogous radical exchange reactions between tyrosine and cysteine residues account for the catalytic activity of ribonucleotide reductases (51).

According to models of the three-dimensional structure of α_1m, Cys-34 is located on a large ω-1 flexible loop (22). This would make it accessible to oxidants that bind to α_1m. Furthermore, it is likely that the thiol interacts with adjacent lysyl residues, because it was recently shown that the catalytic reductase properties of α_1m are dependent on Cys-34 as well as the lysyl residues, Lys-92, Lys-118, and K130A (8). The positively charged lysyl residues may form ionic interactions with the thiolate and consequently lower its pK_a. This would facilitate the ability of the Cys-34 thiol to be oxidized and reduce compounds, such as ABTS radicals (Fig. 12).

It has been known for more than 30 years that α_1m is modified by extremely heterogeneous yellow-brown chromophores. These have been studied extensively, and it was reported previously that the Cys-34 side chain (20) and several lysyl side chains (21) of α_1m isolated from urine or amniotic fluid (29) were modified. In the first report, the modifications could not be identified, and in the second report the sizes of some of the modifications were determined to be 112, 206, and 282 mass units. In the third report, they were structurally identified as derived from the tryptophan metabolite kynurenine. Furthermore, α_1m has been shown to react with hemoglobin and heme (8, 27, 52), and it was hypothesized that the chromophores are degradation products of protoporphyrin (27, 36). In this paper, we have shown that *in vitro* reaction of α_1m with ABTS radical yields purple modifications on at least two tyrosyl residues, and these could be identified as fragments of ABTS.

Thus, a picture emerges of the lipocalin reacting with various organic radicals by reduction and covalent adduction to several of its side chains. A potential physiological function of α_1m could be for it to act as a "radical sink" via its radical reductase and scavenging activities. α_1m is found in all extracellular fluids in levels similar to the plasma concentration (*i.e.* around 2 μM) (53), which we have shown to display significant radical reduction and scavenging activity. In support of this proposal, we found that α_1m was able to prevent an increase in fluorescence of oxidation products of the dipeptide Gly-Tyr. This and related peptides are oxidized by peroxidases to radical species (45). Tyrosyl radicals and oxidation products of tyrosine, such as dopa, are known to promote oxidation in biological systems (54, 55). The most plausible explanation for the action of α_1m is that it reduced either tyrosyl radicals or a related oxidant product when Gly-Tyr was oxidized by lactoperoxidase. We are currently investigating the mechanisms by which α_1m prevents the fluorescence changes associated with oxidation of Gly-Tyr, and

the objects of future studies should be to identify as many as possible of its targets in normal and pathological conditions and to characterize the reaction mechanisms in detail.

REFERENCES

1. Flower, D. R. (1996) *Biochem. J.* **318,** 1–14
2. Åkerström, B., Flower, D. R., and Salier, J.-P. (2000) *Biochim. Biophys. Acta* **1482,** 1–8
3. Urade, Y., and Hayaishi, O. (2000) *Biochim. Biophys. Acta* **1482,** 259–271
4. Hieber, A. D., Bugos, R. C., and Yamamoto, H. Y. (2000) *Biochim. Biophys. Acta* **1482,** 84–91
5. Ekström, B., Peterson, P. A., and Berggård, I. (1975) *Biochem. Biophys. Res. Commun.* **65,** 1427–1433
6. Åkerström, B., and Lögdberg, L. (1990) *Trends Biochem. Sci.* **15,** 240–243
7. Åkerström, B., and Lögdberg, L. (2006) *Lipocalins* (Åkerström, B., Borregaard, N., Flower, D. R., and Salier, J.-S., eds) pp. 110–120, Landes Bioscience, Georgetown, TX
8. Allhorn, M., Klapyta, A., and Åkerström, B. (2005) *Free Radic. Biol. Med.* **38,** 557–567
9. Tejler, L., and Grubb, A. O. (1976) *Biochim. Biophys. Acta* **439,** 82–94
10. Pervaiz, S., and Brew, K. (1985) *Science* **228,** 335–337
11. Kaumeyer, J. F., Polazzi, J. O., and Kotick, M. P. (1986) *Nucleic Acids Res.* **14,** 7839–7850
12. Larsson, J., Wingårdh, K., Davies, J. R., Lögdberg, L., Strand, S. E., and Åkerström, B. (2001) *J. Lab. Clin. Med.* **137,** 165–175
13. Bouic, P., Vincent, C., and Revillard, J.-P. (1984) *Histochem. J.* **16,** 1311–1324
14. Ødum, L., and Nielsen, H. W. (1994) *Histochem. J.* **26,** 799–803
15. Berggård, T., Oury, T. D., Thørgersen, I. B., Åkerström, B., and Enghild, J. J. (1998) *J. Histochem. Cytochem.* **46,** 887–893
16. Berggård, T., Enghild, J. J., Badve, S., Salafia, C. M., Lögdberg, L., and Åkerström, B. (1999) *Am. J. Reprod. Immunol.* **41,** 52–60
17. Lögdberg, L., Åkerström, B., and Badve, S. (2000) *J. Histochem. Cytochem.* **48,** 1545–1552
18. Sanchez, D., Martinez, S., Lindqvist, A., Åkerström, B., and Falkenberg, C. (2002) *Mech. Dev.* **117,** 293–298
19. Ekström, B., and Berggård, I. (1977) *J. Biol. Chem.* **252,** 8048–8057
20. Escribano, J., Grubb, A., Calero, M., and Mendez, E. (1991) *J. Biol. Chem.* **266,** 15758–15763
21. Berggård, T., Cohen, A., Persson, P., Lindqvist, A., Cedervall, T., Silow, M., Thøgersen, I. B., Jönsson, J.-Å., Enghild, J. J., and Åkerström, B. (1999) *Protein Sci.* **8,** 2611–2620
22. Villoutreix, B., Åkerström, B., and Lindqvist, A. (2000) *Blood Coagul. Fibrinol.* **11,** 261–275
23. Lögdberg, L., and Åkerström, B. (1981) *Scand. J. Immunol.* **13,** 383–390
24. Méndez, E., Fernández-Luna, J. L., Grubb, A., and Leyva-Cobián, F. (1986) *Proc. Natl. Sci. Acad. U. S. A.* **88,** 1472–1475
25. Wester, L., Michaelsson, E., Holmdahl, R., Olofsson, T., and Åkerström, B. (1998) *Scand. J. Immunol.* **48,** 1–7
26. Santin, M., and Cannas, M. (1999) *Scand. J. Immunol.* **50,** 289–295
27. Allhorn, M., Berggård, T., Nordberg, J., Olsson, M. L., and Åkerström, B. (2002) *Blood* **99,** 1894–1901
28. Allhorn, M., Lundqvist, K., Schmidtchen, A., and Åkerström, B. (2003) *J. Investig. Dermatol.* **121,** 640–646
29. Sala, A., Campagnoli, M., Perani, E., Romano, A., Labo, S., Monzani, E., Minchiotti, L., and Galliano, M. (2004) *J. Biol. Chem.* **279,** 51033–51041
30. Ishii, T., Iwahashi, H., Sugata, R., and Kido, R. (1992) *Arch. Biochem. Biophys.* **294,** 616–622
31. Okuda, S., Nishiyama, N., Saito, H., and Katsuki, H. (1996) *Proc. Natl. Acad. Sci. U. S. A.* **93,** 12553–12558
32. Vazquez, S., Garner, B., Sheil, M. M., and Truscott, R. J. W. (2000) *Free Radic. Res.* **32,** 11–23
33. Pawlak, D., Pawlak, K., Malyszko, J., Mysliwiec, M., and Buczko, W. (2001)

Int. Urol. Nephrol. **33,** 399–404

34. Olsson, M. G., Allhorn, M., Olofsson, T., and Åkerström, B. (2007) *Free Radic. Biol. Med.* **42,** 842–851
35. Miller, N. J., and Rice-Evans, C. A. (1997) *Free Radic. Res.* **26,** 195–199
36. Kwasek, A., Osmark, P., Allhorn, A., Lindqvist, A., Åkerström, B., and Wasylewski, Z. (2007) *Protein Expression Purif.* **53,** 145–152
37. Berggård, T., Thelin, N., Falkenberg, C., Enghild, J. J., and Åkerström, B. (1987) *Eur. J. Biochem.* **245,** 676–683
38. Åkerström, B., Bratt, T., and Enghild, J. J. (1995) *FEBS Lett.* **362,** 50–54
39. Wester, L., Johansson, M. U., and Åkerström, B. (1997) *Protein Expression Purif.* **11,** 95–103
40. Pe, R., Pellegrini, N., Proteggente, A., Pannala, A., Yang, M., and Rice-Evans, C. A. (1999) *Free Radic. Biol. Med.* **26,** 1231–1237
41. Shin, T., Murao, S., and Matsumura, E. (1987) *Anal. Biochem.* **166,** 380–388
42. Childs, R., and Bardsley, W. G. (1975) *Biochem. J.* **145,** 93–103
43. Laemmli, U. K. (1970) *Nature* **227,** 680–685
44. Madsudaira, P. (1987) *J. Biol. Chem.* **262,** 10035–10038
45. Winterbourn, C. C., Parsons-Mair, H. N., Gebicki, S., Gebicki, J. M., and Davies, M. J. (2004) *Biochem. J.* **389,** 785–795
46. Arnao, M. B., Casas, J. L., del Rio, J. A., Acosta, M., and Garcia-Canovas, F. (1990) *Anal. Biochem.* **185,** 335–338
47. Aliaga, C., and Lissi, E. A. (2000) *Can. J. Chem.* **78,** 1052–1059
48. Prutz, W. A., Butler, J., Land, E. J., and Swallow, A. J. (1986) *Free Radic. Res. Commun.* **2,** 69–75
49. Davies, M. J., and Dean, R. T. (1997) *Radical Mediated Protein Oxidation From Chemistry to Medicine*, p. 95, Oxford University Press, Oxford
50. Buettner, G. R. (1993) *Arch. Biochem. Biophys.* **300,** 535–543
51. Stubbe, J., and Riggs-Gelasco, P. (1998) *Trends Biochem. Sci.* **23,** 438–443
52. Larsson, J., Allhorn, M., and Åkerström, B. (2004) *Arch. Biochem. Biophys.* **432,** 196–204
53. DeMars, D. D., Katzmann, J. A., Kimlinger, T. K., Calore, J. D., and Tracy, R. P. (1989) *Clin. Chem.* **35,** 766–772
54. Heinecke, J. W. (2002) *Toxicology* **177,** 11–22
55. Pattison, D. I., Dean, R. T., and Davies, M. J. (2002) *Toxicology* **177,** 23–37